Novel Luminescent Sensor for Ice Temperature Measurement

Joseph Gonzales[1], Masafumi Yamazaki[1], Owen Duffy[1], Hirotaka Sakaue[1]

[1] University of Notre Dame, IN, USA

jgonza21@nd.edu, myamazak@nd.edu, oduffy@nd.edu, hsakaue@nd.edu

Abstract— **A novel luminescent sensor that provides spatially and temporally resolved temperature information within ice is developed. The purpose of the sensor is to be able to study the fundamentals of freezing, melting, and ice removal systems in a controlled lab environment, to promote better systems for use in industry. The sensor relies on the luminescent output of pyranine, which produces two luminescent peaks within ice. The ratio of these peaks can be quantitatively related to temperature in both the solid and liquid phases. The sensor is calibrated using a spectrometer, and exhibits a temperature sensitivity of -9.2±0.1%K-1 for the solid phase and 0.8±0.1%K-1 for the liquid phase The sensor is then applied to three separate experimental demonstrations. The first is surface temperature measurements of a heated thin rectangular prism. The second and third are internal temperature measurements of a wedge and cylinder in forced convection. All experimental measurements are qualitatively in agreement with expected heat transfer characteristics.**

Keywords— ***hydroxypyrene, spatiotemporal, temperature, phase change, self-referencing***

I. INTRODUCTION

Ice formation, the freezing process, and ice melting and removal are complex phenomena that are relevant to a large number of industries and applications [1-4]. However, despite the fact that this area of study is so far-reaching, the number of tools to study fundamental ice dynamics is limited. This is especially true concerning measurement of phase change and internal temperature measurements. Many attempts to study icing are done using computational models, in bulk analysis, and analysis of how icing affects given properties, such as structural stability and aircraft performance [3-5]. While computational models can provide useful insights into ice dynamics, new simulation tools are constantly under development. These new tools require high-quality temporally and spatially resolved experimental data to validate them.

Certain techniques can be used to measure the surface temperature of ice, such as the use of infrared camera technology, but this is limited to surface information and can exhibit low signal to noise ratios due to the low radiation output of ice. Newer techniques utilize the infrared absorption of ice to measure temperature [5], but this can require complex equipment and is unable to easily measure rapid changes in temperature. Other methods such as the use of thermocouples and other temperature probes provide highly accurate temporally resolved temperature data. However, these methods are intrusive and generally limited to single point measurements.

In contrast, luminescent sensors provide a workaround for these issues, with spatially resolved information, high sensitivity, and high signal to noise ratio at low temperatures. As an optical method, luminescent sensors are non-intrusive, and can provide temporally resolved information. At a fundamental level, luminescent sensors relate the luminescent output of a molecule to some quantity of interest, such as pH, pressure, or temperature [6]. Currently, chemical luminescent sensors are used in a variety of applications to sense temperature, and are typically used to measure surface temperature or the temperature within a solution [7-10]. However, luminescent sensors are limited only by optical access, and so the transparency of ice provides a unique opportunity for the use of such sensors to measure internal temperature and phase changes. Such a sensor allows for better insight into a number of complex icing phenomena, as well as validation of computational icing models.

This work describes the development and characterization of the sensor, as well as a simple validation test using various geometries to demonstrate internal heating measurements.

II. NOVEL SENSOR DYNAMICS

The novel luminescent sensor relies on hydroxypyrene, also known as pyranine, a pH sensitive molecule to extract temperature information from within ice. The use of pyranine as a luminescent sensor is well documented in the literature and is generally used to study pH in biological applications [11-13]. When dissolved in water and excited by 365nm light, the pyranine molecule emits light with two distinct luminescent peaks, one at 441nm and one at 511nm. These peaks are related to the two different forms of pyranine which exist in solution [13]. The protonated form emits light with a peak at 441nm and the deprotonated form emits light with a peak at 511nm. The luminescent spectrum of pyranine dissolved in distilled water is shown in Figure 1.
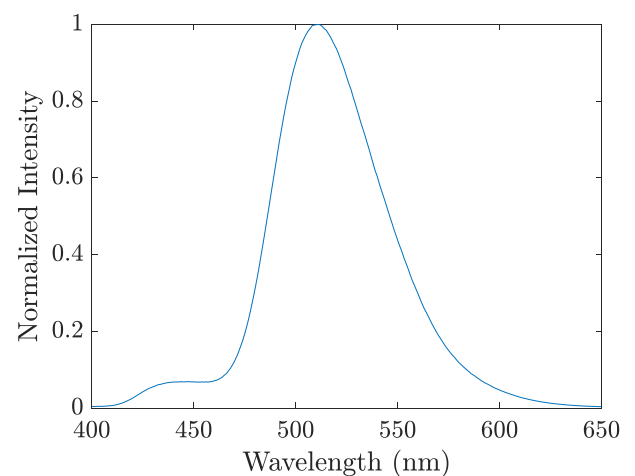
Fig. 1: The luminescent spectrum of pyranine dissolved in distilled water at 20ºC is shown. There are two peaks, one at 441nm, and a much higher intensity peak at 511nm.

As shown, the peak at 441nm is substantially lower in intensity than the peak at 511nm for liquid water at 20ºC. This is because pyranine is a weak acid, and when dissolved in water, tends to deprotonate. The emission from the deprotonated form of pyranine is thus dominant. However, the ratio of the 441nm and the 511nm peaks is a function of solution makeup and can be used to extract temperature information in both the solid and liquid phases [14].

A luminescent temperature sensor was created according to the recipe in [14], and characterized using spectral analysis. A small sample of luminescent water was placed on a temperature controller. The temperature was varied between -15º and 20ºC, and spectral measurements were collected at various temperature points in both the liquid and solid phases. A schematic of the temperature calibration setup is shown in Figure 2.
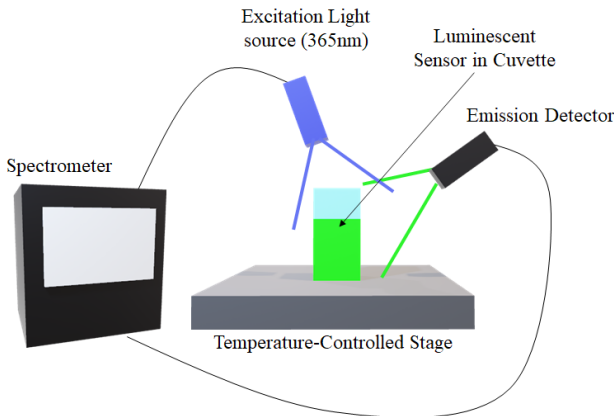

Fig. 2: The schematic of the temperature calibration setup using spectrometer and temperature-controlled stage is shown. 0.5mL of the luminescent ice sensor was placed onto the temperature controlled and excited by 365nm light.

The spectra emitted by the luminescent ice sensor at various temperatures in the solid and liquid phases are shown in Figures 3 and 4 respectively. As shown, there is a clear change in the luminescent intensities at 441 and 511nm with changing temperature. This is true in both the solid and liquid phases.
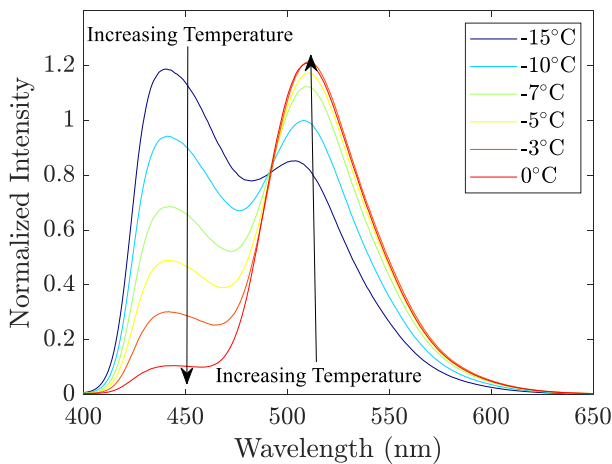

Fig. 3: The spectra of the luminescent ice sensor in the ice phase for various temperatures is shown. The peak at 441nm, which is visible as blue in color, decreases with increasing temperature. The peak at 511nm, which is green in color, increases with temperature.
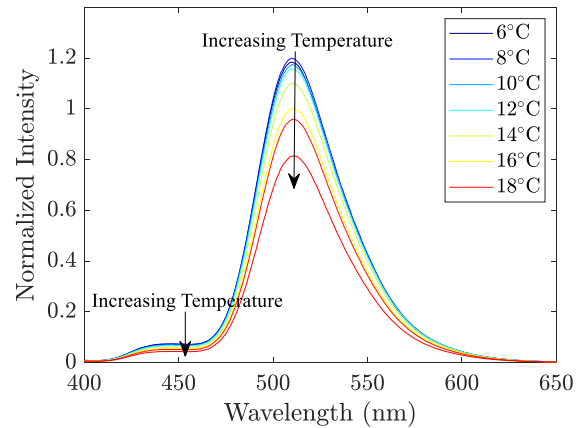

Fig. 4: The spectra of the luminescent sensor in the liquid phase for various temperatures is shown. Both the peak at 441nm and at 511nm decrease with increasing temperature. However, the response of the peak at 441nm is less sensitive to temperature effects in the liquid phase than the peak at 511nm.

The ratio between the intensities at the 441nm and the 511nm peaks was taken to determine a calibration curve for the temperature in both the liquid and solid phases. Taking the ratio of the deprotonated peak intensity (511nm), I_D, over the protonated peak intensity (411nm), I_p, gives a linear trend in the solid phase as shown in Figure 5. Taking the inverse of this, I_P/I_D, gives a linear trend in the liquid phase.
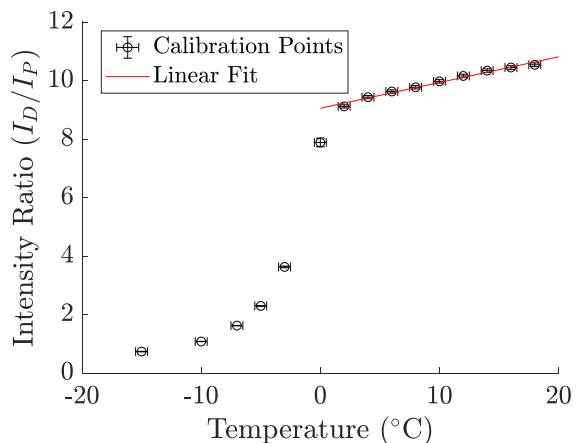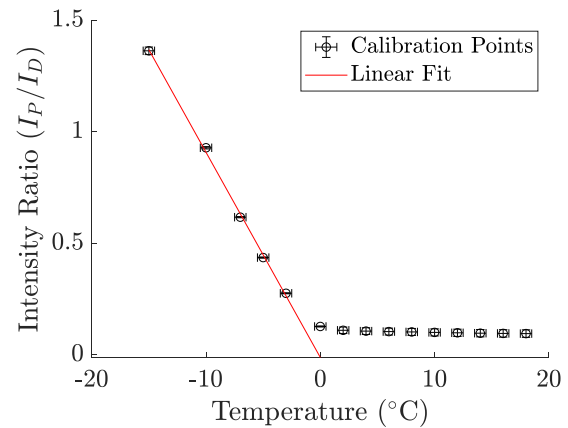
Fig. 5: Ratio of peak intensities as a function of temperature for the luminescent sensor in the solid phase (I_P/I_D, top) liquid phase (I_D/I_P, bottom)

The sensitivity of the luminescent temperature sensor is defined as the slope of these linear fits and is $-9.2\pm0.1\%\,K^{-1}$ for the solid phase and $0.8\pm0.1\%\,K^{-1}$ for the liquid phase. These calibration curves give a quantitative relationship between overall luminescent output of the sensor and its global temperature profile. Because the two peaks are distinct from one another in terms of visible color, a spectrometer is not necessary for temperature measurement. Instead, a color camera is able to separate the protonated and deprotonated peak emissions into blue and green channels, respectively. In this way, a color camera can be used to measure dynamic changes in temperature and phase by taking the ratio of the intensity outputs from its blue and green channels. Examples of this type of measurement are described in the following section.

III. EXPERIMENTAL DEMONSTRATION

Three experimental demonstrations were conducted using the novel luminescent sensor. The first was a measurement of the surface temperature of a thin rectangular prism as it was heated. The second and third were measurements of the internal temperature of an ice wedge and ice cylinder, respectively. All experiments were conducted using a 365nm LED illumination source from Thorlabs and a Photron high-speed color camera. An *a priori* temperature calibration similar to that conducted in Section II was performed using the high-speed color camera instead of the spectrometer. This calibration was used to convert between images captured by the camera and temperature maps.

A. Rectangular Prism heating

A thin rectangular prism with dimensions 90mm x 10mm x 1mm was created out of ice using the recipe in [14]. The ice rectangular prism was insulated on two sides using plastic rods and was placed onto a large aluminum block. Both the aluminum block and the ice rectangular prism were cooled to an initial temperature of -20°C. The ice rectangular prism was excited by the 365nm light source and images of the system were captured by the high-speed color camera at a frequency of 50Hz. The right side of the aluminum block was then heated to a temperature of approximately 70°C. A schematic of the experimental setup is shown in Figure 6 and images of the ice rectangular prism during the experiment as shown in Figure 7.
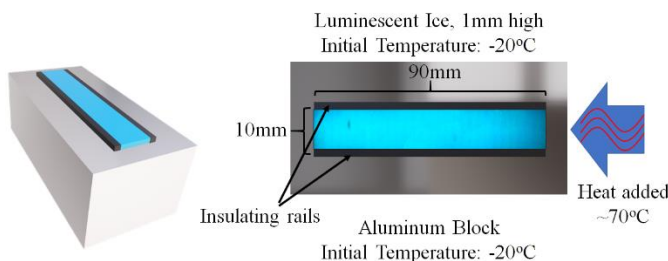

Fig. 6: A schematic of the heated rectangular prism experimental setup is shown.
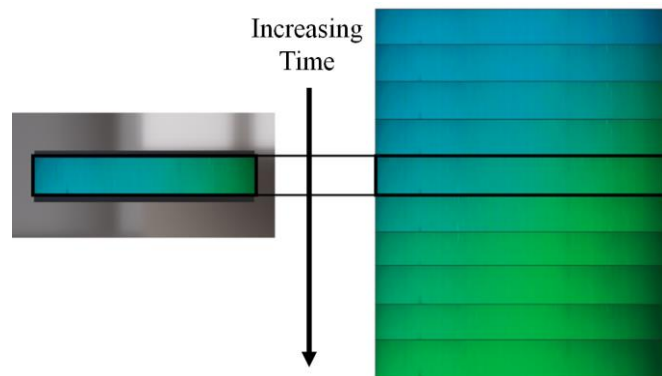

Fig. 7: Images from the heated rectangular prism experiment are shown, arranged in increasing time order from top to bottom. The color of the sensor gradually shifts from blue to green during the experiment, showing the increase in temperature along the rectangular prism.

As shown, the color of the sensor continually changes from blue to green during the experiment. The ratio intensity in the blue and green channels of the color camera was used to convert the images to temperature maps of the rectangular prism. The temperature map at various times during the experiment is shown in Figure 8.
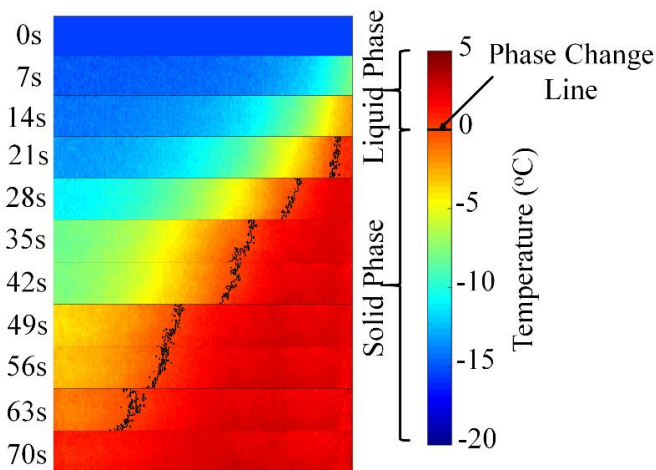

Fig. 8: Temperature profiles of the ice rectangular prism during heating are shown. There is a clear increase in temperature from right to left over time, and melting over the prism is visible. This melting line is indicated in black on the temperature maps.

The behavior of the temperature map agrees well with expectations, as the temperature increases gradually from right to left, as the right side of the ice is heated. In addition, during the experiment, the ice prism melted. The melting front was detected by using the ratio of the blue and green channels and the *a priori* calibration of the sensor. The angle of the melting front is a product of non-uniform heating of the aluminum block and melting water running over the rest of the ice prism.

B. Wedge Heating

In order to measure the change in internal temperature of an ice object as it is exposed to forced convection, a 30° half angle wedge was created. The wedge was formed by creating a thin layer of luminescent ice between two larger layers of pure water ice. The transparency of the pure water ice allowed for optical measurement of the internal luminescent layer. The

wedge was mounted on a plastic insulating sting and exposed to 50°C air. A schematic of the wedge and its dimensions is shown in Figure 9.
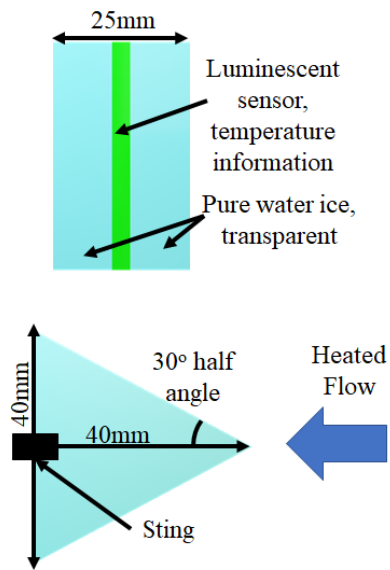

Fig. 9: A schematic of the wedge heating experiment is shown. The wedge model was created by placing a thin layer of the luminescent temperature sensor between blocks of pure water ice. This allowed for measurement of just the internal temperature of the wedge, as opposed to the surface temperature.

During the experiment, images were captured at a frequency of 50 Hz using the color camera. The images were converted to temperature maps using the *a priori* temperature calibration. Images of the wedge at different times during the experiment are shown in Figure 10.
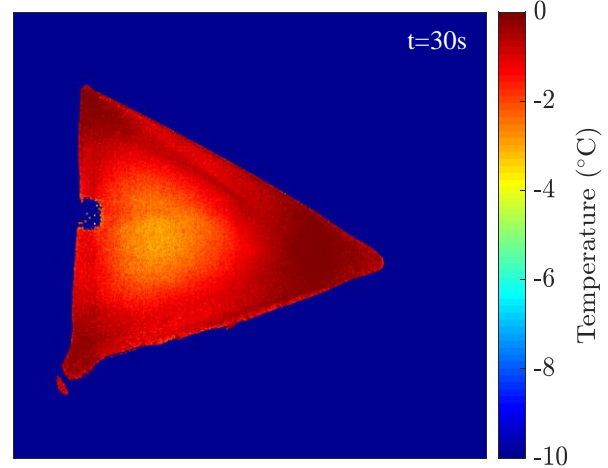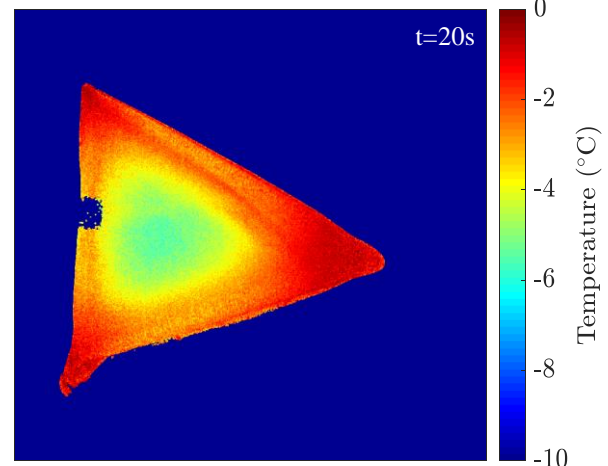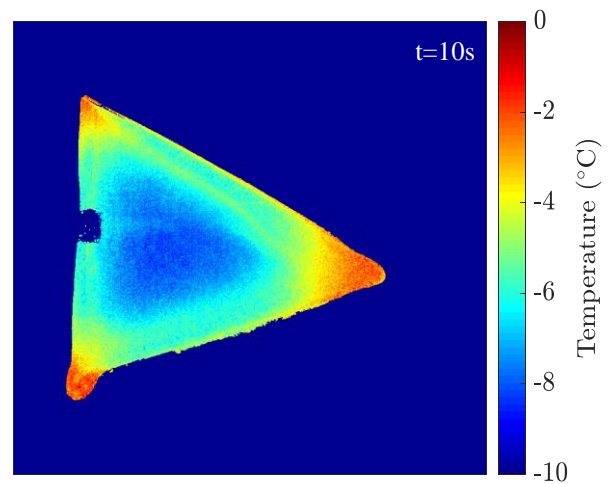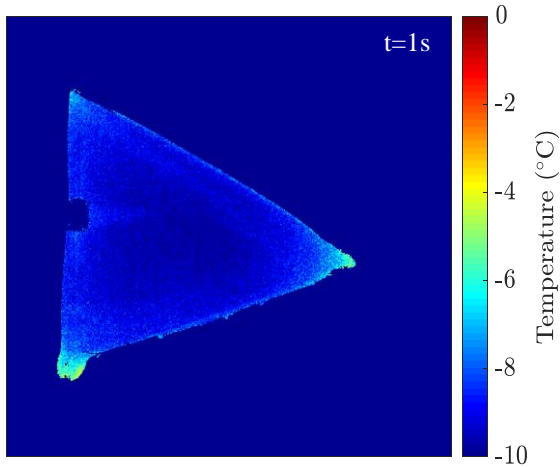

Fig. 10: Time progression of temperature maps of the heated wedge are shown for t=1, 10, 20 and 30 seconds. Melting of the wedge is clearly visible on the bottom left of the image.

As shown, the wedge object heats from the outside in, demonstrating that the sensor is measuring the internal temperature of the wedge, not the surface temperature. The areas of highest heating are the corners of the model, which is expected, as these areas have the highest exposed surface area per unit mass of the entire model. Melting of the wedge is clearly visible in both the deformation of the model and the temperature maps.

C. Cylindrical Heating

An additional experiment was conducted using a cylinder heated from the top with air at a temperature of 50°C. Again, the cylinder was created by forming a thin layer of luminescent ice between two layers of pure water ice. A schematic of the cylinder and its dimensions are shown in Figure 11.
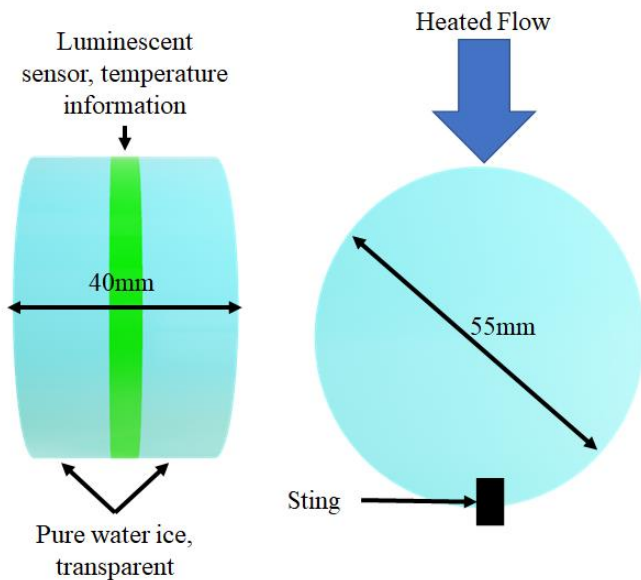

Fig. 11: A schematic of the cylinder heating experiment is shown. The cylinder model was created by placing a thin layer of the luminescent temperature sensor between blocks of pure water ice. This allowed for measurement of just the internal temperature of the cylinder, as opposed to the surface temperature.

During the experiment, images were captured at a frequency of 50 Hz using the color camera. The images were converted to temperature maps using the *a priori* temperature calibration. Images of the cylinder at different times during the experiment are shown in Figure 12.
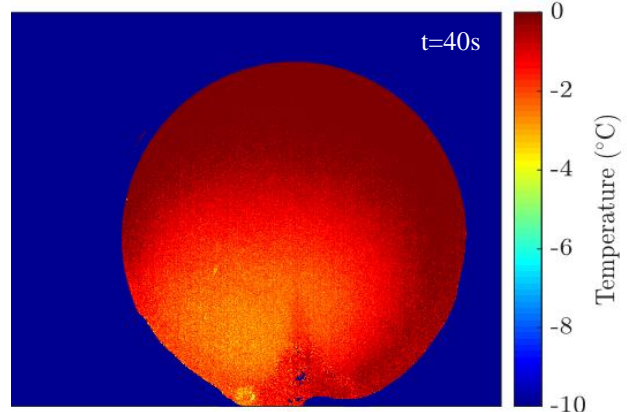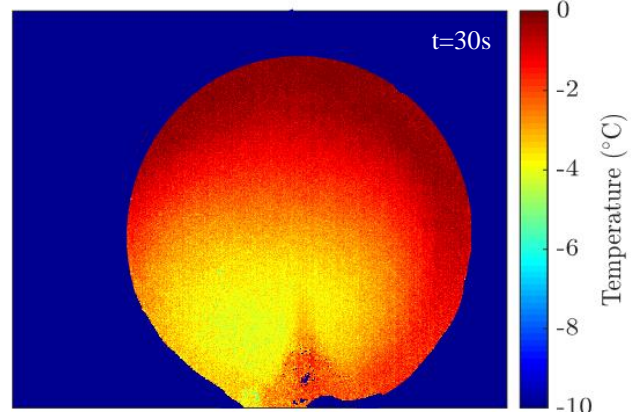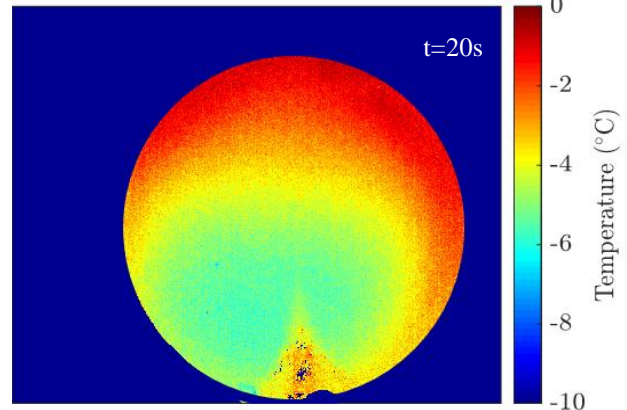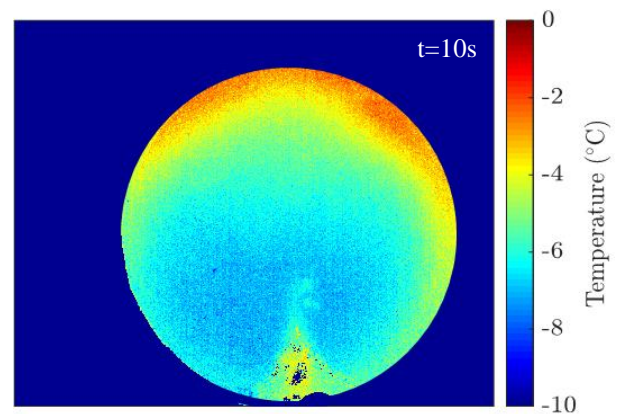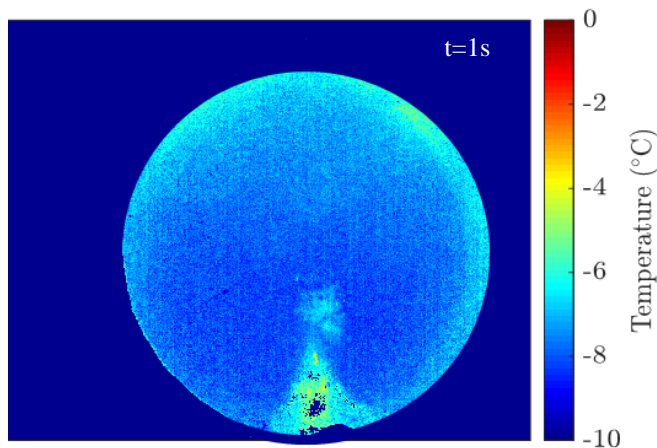

Fig. 12: Images of the time progression of temperature maps of the heated cylinder are shown for t=1, 10, 20, 30 and 40 seconds. Melting is visible for the images taken at 30 and 40 seconds at the bottom of the cylinder.

As shown, the cylinder heats most rapidly from the top stagnation point, which is consistent with heat transfer for a non-rotating cylinder. The temperature profile is plotted as a function of angular position as shown in Figure 13.
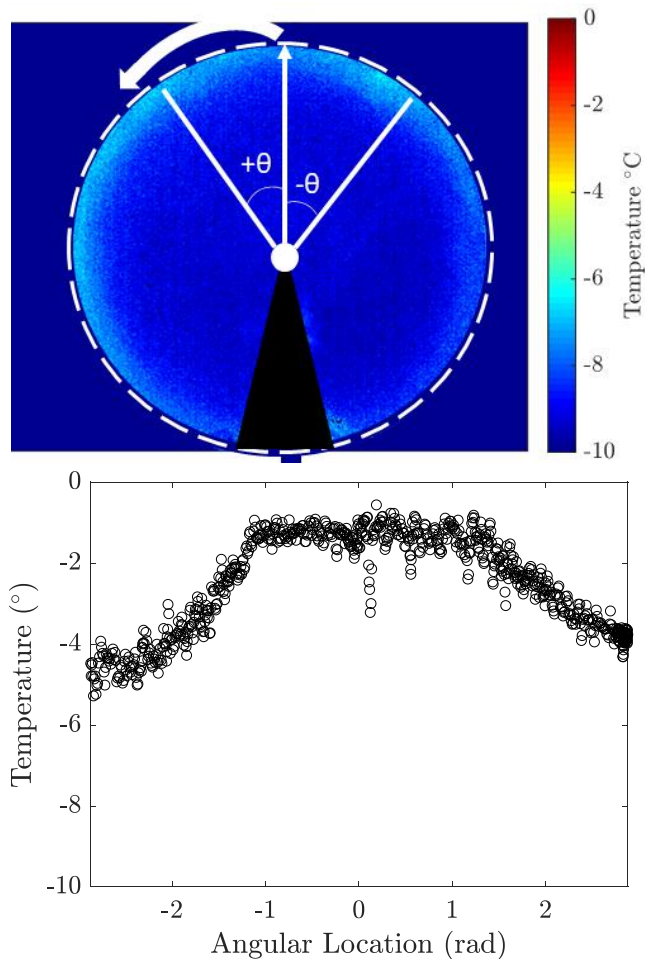

Fig. 13: (Above) A schematic showing the definition of angle θ and the total angle range plotted for the cylinder. The bottom portion of the cylinder was ignored as the temperature data is corrupted by the presence of the sting. (Below) Plot of surface temperature of cylinder as function of angle around cylinder.

The initial temperature of the cylinder was uniform at -10°C. It was assumed that the heating of the cylinder due to conduction is much more rapid than the internal heat transfer due to conduction based on the rate of change of the measured temperature field. Thus, the temperature profile of the cylinder is an approximate estimate of the heat transfer as a function of angle around the cylinder. Figure 13 is qualitatively consistent with what is predicted by [15]. Differences between the exact analytical prediction and experimental observations are due to phase change and ablative effects as the cylinder melts, as well as the assumption that internal heat transfer occurs more slowly than convective heating.

IV. DISCUSSION

The novel luminescent temperature sensor embedded within ice is able to quantitatively relate luminescent output to a spatially and temporally resolved temperature map. The sensitivity of the novel sensor is substantially higher than most currently available luminescent sensors. The sensor is dynamic, and can be used to measure both ice surface temperature and internal temperature, as well as phase change. The sensor itself is versatile, and can be applied to any geometry than can be created out of ice. Because the sensor relies on the ratio between two luminescent outputs, it can be used in cases where the light source of the object of interest is in motion, or is changing in shape. This is done by using the motion-capturing technique developed by Sakaue, *et al.* [16].

As with all luminescent sensors, the performance of the luminescent temperature sensor embedded within ice can be changed by modifying the recipe used to create it. Further investigation must be conducted in order to determine the optimal sensor recipe in terms of both sensitivity and overall intensity ratio. The mixture used to create the sensor may also have an impact on the water and ice properties, including density, freezing point, surface tension in the liquid phase, and yield stress in the solid phase. A thorough study must be conducted to determine the impact of the luminescent sensor mixture on solution and ice properties.

V. CONCLUSIONS

A novel luminescent temperature sensor was created using pyranine. The sensor was embedded within ice and was used to measure the surface temperature of and internal temperature within ice. The sensor exhibits temperature sensitivity of $-9.2\pm0.1\%\,\mathrm{K}^{-1}$ between $-15°$ and $0°C$ within the ice phase and $0.8\pm0.1\%\,\mathrm{K}^{-1}$ between $0°C$ and $20°C$ within the liquid phase. This sensor can be used to provide spatially and temporally resolved temperature information on the surface of melting and ablating materials, and can be applied to measure the internal temperature of objects. Further studies using this luminescent sensor will be conducted on more complex geometries, more complicated icing conditions, and various flow and heat transfer phenomena.

REFERENCES

[1] G. A. Longo and C. Zilio, "Experimental measurement of thermophysical properties of oxide–water nano-fluids down to ice-point", *Experimental Thermal and Fluid Science* vol. 35 pp. 1313–1324, 2011 doi:10.1016/j.expthermflusci.2011.04.019.

[2] S. M. Patel, C. Bhugra, and M. J. Pikal, "Reduced pressure ice fog technique for controlled ice nucleation during freeze-drying", *AAPS PharmSciTech*, vol. 10, pp. 1406, 2009, doi:10.1208/s12249-009-9338-7.

[3] G. Zuo, Y. Dou, and R. Lei, "Discrimination algorithm and procedure of snow depth and sea ice thickness determination using measurements of the vertical ice temperature profile by the ice-tethered buoys", *Sensors* vol. 18, pp.4162, 2018, doi:10.3390/s18124162.

[4] B. Sass, "A numerical model for prediction of road temperature and ice", *Journal of Applied Meterology and Climatology*, vol. 31, pp. 1499–1506, 1992, doi:10.1175/1520-0450(1992)031<1499:ANMFPO>2.0.CO;2.

[5] W. M. Grundy and B. Schmitt, "The temperature-dependent near-infrared absorption spectrum of hexagonal h2o ice", *Journal of Geophysical Research: Planets* vol. 103, pp. 25809–25822, 1998, doi: 10.1029/98JE00738.

[6] T. Liu and J. Sullivan, *Pressure and Temperature Sensitive Paints*, Springer-Verlag , 2005.

[7] B. Dong, B. Cao, Y. He, Z. Liu, Z. Li, and Z. Feng, "Temperature sensing and in vivo imaging by molybdenum sensitized visible upconversion luminescence of rare-earth oxides", *Advanced Materials,* vol. 24, pp. 1987–1993 (2012). doi:10.1002/adma.201200431.

[8] J. Zhou, H. Li, H. Zhang, H. Li, W. Shi, and P. Cheng, "A bimetallic lanthanide metal–organic material as a self-calibrating color-gradient luminescent sensor", *Advanced Materials*, vol. 27, pp.7072–7077, 2015, doi:10.1002/adma.201502760.

[9] H. Peng, M. Stich, J. Yu, L. Sun, L. Fischer, and O. Wolfbeis, "Luminescent europium(iii) nanoparticles for sensing and imaging of temperature in the physiological range", *Advanced Materials*, vol. 22, pp. 716–719, 2010, doi:10.1002/adma.200901614.

[10] D. Gong, T. Cao, S. Han, X. Zhu, A. Iqbal, W. Liu, W. Qin, and H. Guo, "Fluorescence enhancement thermoresponsive polymer luminescent sensors based on bodipy for intracellular temperature", *Sensors and Actuators B: Chemical*, vol. 252, pp. 557–583, 2017, doi: 10.1016/j.snb.2017.06.041.

[11] K. A. Giuliano and R. J. Gillies, "Determination of intracellular ph of balbc-3t cells using the fluorescence of pyranine", *Analytical Biochemistry* vol. 167, pp. 362–371, 1987, doi:10.1016/0003-2697(87)90178-3.

[12] O. S. Wolfbeis, E. Furlinger, H. Kroneis, and H. Marsoner, "A study on fluorescent indicators for measuring near neutral physiological ph-values", *Analytical Chemistry*, vol. 314, pp. 119–124, 1983.

[13] D. Willoughby, R. C. Thomas, and C. J. Schwiening, "Comparison of simultaneous ph measurements made with 8-hydroxypyrene-1,3,6-trisulphonic acid (hpts) and ph-sensitive microelectrodes in snail neurones", *Instruments and Techniques*, vol. 426, pp. 615–622, 1998.

[14] J. Gonzales and H. Sakaue, "Novel optical temperature and phase change sensor based on the response of hydroxypyrene to sucrose in water ice", *Sensors and Actuators A: Physical*, (under review)

[15] D. Maillet, A. Degiovanni, and R. Pasquetti, "Inverse Heat Conduction Applied to the Measurement of Heat Transfer Coefficient on a Cylinder: Comparison Between Analytical and a Boundary Element Technique", *Journal of Heat Transfer*, vol. 113, pp. 549-557, 1991.

[16] H. Sakaue, K. Miyamoto and T. Miyazaki, "A motion-capturing pressure-sensitive paint method", *Journal of Applied Physics*, vol. 113, pp. 084901, 2013, doi:10.1063/1.4792761.